CHEMISTRY
A European Journal

A Journal of ChemPubSoc Europe

www.chemeurj.org

2018-24/00

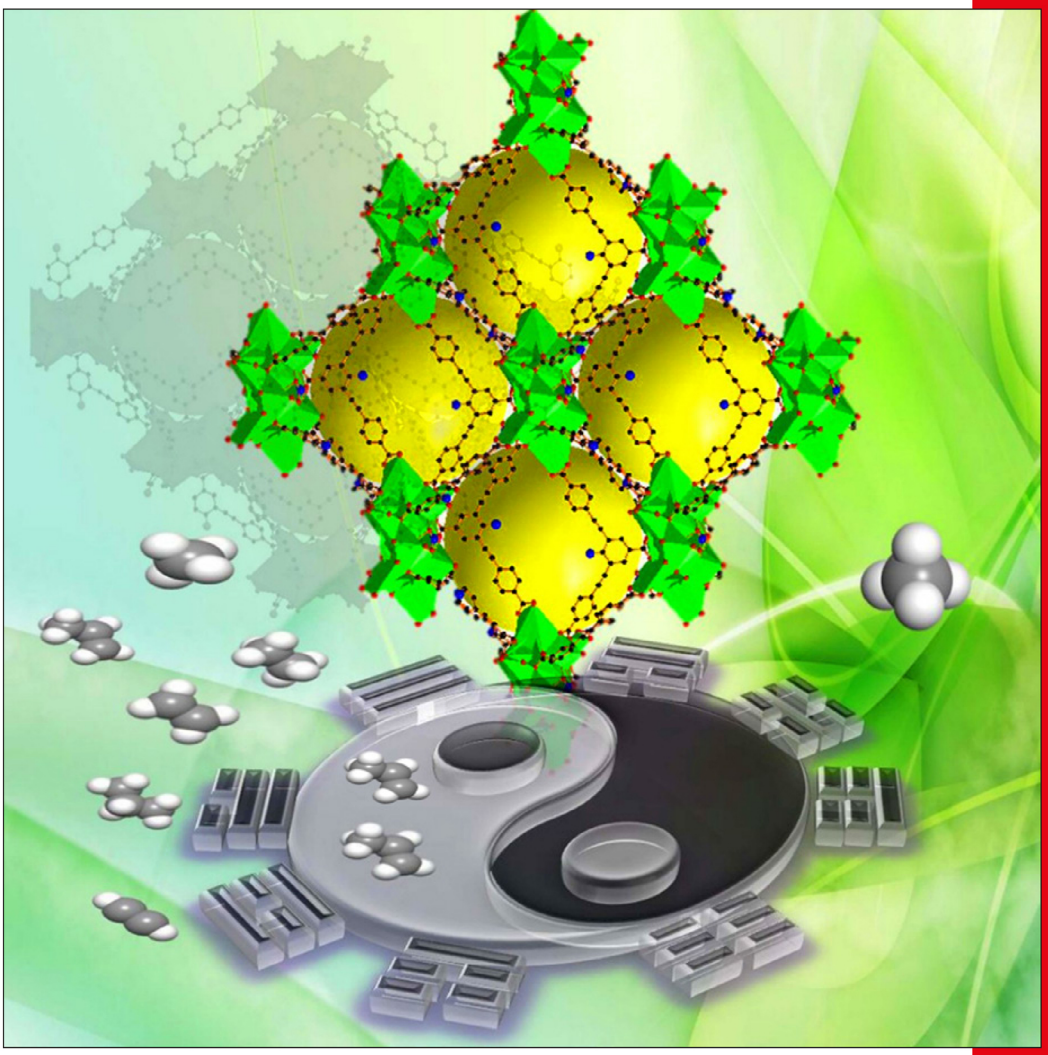

Cover Feature:
L. Zhang, D. Sun et al.
An Amino-Functionalized Metal-Organic Framework, Based on a Rare $Ba_{12}(COO)_{18}(NO_3)_2$ Cluster, for Efficient $C_3/C_2/C_1$ Separation and Preferential Catalytic Performance

Supported by ACES Asian Chemical Editorial Society

WILEY-VCH

COVER PICTURE

W. Fan, Y. Wang, Q. Zhang, A. Kirchon, Z. Xiao, L. Zhang, F. Dai, R. Wang, D. Sun**

■■ – ■■

An Amino-Functionalized Metal-Organic Framework, Based on a Rare $Ba_{12}(COO)_{18}(NO_3)_2$ Cluster, for Efficient $C_3/C_2/C_1$ Separation and Preferential Catalytic Performance

An amino-functionalized and $Ba_{12}(COO)_{18}(NO_3)_2$-based microporous metal – organic framework (UPC-33) has been synthesized. UPC-33 displays not only permanent porosity, but also high adsorption heat of CO_2 and selectivity of CO_2/CH_4. In addition, UPC-33 exerts a high separation selectivity for C_3 light hydrocarbons relative to CH_4, and can selectively adsorb C_3H_6 from C_2 hydrocarbons. Based on the above work, the cover depicts a traditional Chinese-style gossip image of UPC-33, which acts as a platform for adsorbing C_3 while separating C_1. More information can be found in the Full Paper by L. Zhang, D. Sun et al. (DOI: 10.1002/chem.201704629).

ChemPubSoc Europe

DOI: 10.1002/chem.201704629

CHEMISTRY A European Journal Full Paper

Metal-organic Frameworks

An Amino-Functionalized Metal-Organic Framework, Based on a Rare $Ba_{12}(COO)_{18}(NO_3)_2$ Cluster, for Efficient $C_3/C_2/C_1$ Separation and Preferential Catalytic Performance

Weidong Fan,[a] Yutong Wang,[a] Qian Zhang,[b] Angelo Kirchon,[a] Zhenyu Xiao,[a] Liangliang Zhang,*[a] Fangna Dai,[a] Rongming Wang,[a] and Daofeng Sun*[a]

Abstract: A barium(II) metal-organic framework (MOF) based on a predesigned amino-functionalized ligand, namely $[Ba_2(L)(DMF)(H_2O)(NO_3)_{1/3}]\cdot DMF\cdot EtOH\cdot 2H_2O$ (UPC-33) [H_3L = 4,4′-((2-amino-5-carboxy-1,3-phenylene)bis(ethyne-2,1-diyl))-dibenzoic acid] has been synthesized. UPC-33 is a 3-dimensional 3,18-connected network with *fcu* topology with a rare twelve-nuclear $Ba_{12}(COO)_{18}(NO_3)_2$ cluster. UPC-33 shows permanent porosity and a high adsorption heat of CO_2 (49.92 kJ mol^{-1}), which can be used as a platform for selective adsorption of CO_2/CH_4 (8.09). In addition, UPC-33 exhibits its high separation selectivity for C_3 light hydrocarbons with respect to CH_4 (228.34, 151.40 for C_3H_6/CH_4, C_3H_8/CH_4 at 273k and 1 bar), as shown by single component gas sorption and selectivity calculations. Due to the existence of $-NH_2$ groups in the channels, UPC-33 can effectively catalyze Knoevenagel condensation reactions with high yield, and substrate size and electron dependency.

Introduction

Porous metal-organic frameworks (MOFs), or coordination polymers, which can be self-assembled from organic linkers and metal ions/clusters directly, have developed rapidly in the fields of chemistry and material science. As a new type of promising adsorbents, MOFs have been intensively investigated for applications in storage and separation of gases, such as H_2, O_2, CH_4, and CO_2.[1–3] The biggest advantage of MOFs over other porous materials such as activated carbon and zeolites is the high surface area, and the tunable chemical and physical properties of the pores.[4–6] MOFs have been recently been studied for light hydrocarbon storage applications.[7,8] For example, **UPC-21** shows a high C_3H_6 and C_3H_8 uptakes of 124.1 and 116.2 cm^3 g^{-1} at 273 K.[9] In addition, MOFs have also been employed as new solid sorbents for the separation of light hydrocarbons.[5,10,11] Several strategies have been adopted, including tailoring pore surface function, tuning pore size and shape, and utilizing structural flexibility, to enhance the efficiency of selective gas separation.[12–14] Among them, the pore sizes and shapes of the MOFs sorbents are of first and foremost importance for their separation performance. The pore size of the adsorbent, which is comparable to or slightly larger than the kinetic diameters of the adsorbate, will significantly promote the separation selectivity of these light hydrocarbons. Thus, the design and synthesis of MOFs with a narrow pores close to 4.4 Å is crucial for their performances in the separation of these light hydrocarbons (C1–C3) as the kinetic diameters range from 3.3 to 4.4 Å.[15] In addition, tailoring pore surface function, such as the immobilization of polar functional groups –OH, $-NH_2$, and/or the formation of charge skeletons, is another effective strategy to improve the efficiency of MOFs separation efficiency based on adsorbate-surface interaction.[16,17] Chen and Zhang explored a series of microporous MOFs with pore and size control for energy adsorption separation of light hydrocarbons.[5] The functional MOF materials, with highly ordered pores, also show great potential for catalytic applications.[18] Thus, Knoevenagel condensation reactions are an efficient way to obtain valuable intermediate chemicals based on C–C coupling. Conventionally, these reactions are catalyzed by homogeneous catalysts. However, due to the low stability and high recovery costs, it is difficult to recover the catalyst. Therefore, it is highly desirable to develop a heterogeneous catalyst having high stability and good recyclability.

In this contribution, we have designed a novel amino functionalized ligand, 4,4′-((2-amino-5-carboxy-1,3-phenylene)bis(ethyne-2,1-diyl))dibenzoic acid (H_3L), and synthesized an amino functionalized metal-organic framework (UPC-33) with an open channel based on a rare $Ba_{12}(COO)_{18}(NO_3)_2$ cluster. The pore

[a] W. Fan, Y. Wang, A. Kirchon, Z. Xiao, L. Zhang, Dr. F. Dai, R. Wang, Prof. D. Sun
State Key Laboratory of Heavy Oil Processing, College of Science
China University of Petroleum (East China)
NO. 66, Changjiang Road West, Qingdao, 266580 (PR China)
E-mail: liangliangzhang@upc.edu.cn
dfsun@upc.edu.cn

[b] Q. Zhang
State Key Laboratory of Catalysis
Dalian Institute of Chemical Physics, Chinese Academy of Sciences
NO. 457, Zhongshan Road, Dalian, 116023 (PR China)

Supporting information and the ORCID identification number(s) for the author(s) of this article can be found under: https://doi.org/10.1002/chem.201704629.

size distribution of UPC-33 is ~4.3 Å, which is close to the kinetic diameter of light hydrocarbons (C1–C3). The amino-functionalized UPC-33 exhibits high selectivity to light hydrocarbons (C3) and CO_2 relative to CH_4 at room temperature. The selectivity of UPC-33 for C_3H_8/CH_4 is comparable to FJI–C1, and higher than that of USTA-35a, or JLU-Liu22.[19–22] Additionally, UPC-33 demonstrates high substrate size and electron dependency catalytic properties for Knoevenagel condensation reactions.

Results and Discussion

Crystal structures of UPC-33

Single crystal X-ray diffraction reveals that **UPC-33** crystallizes in the trigonal system with a space group $R\bar{3}$. The crystallographic data are summarized in Table S1 (Supporting Information) and the selected bond lengths and bond angles of the compound are listed in Table S2. The fundamental building unit of **UPC-33** contains two barium ions, one crystallographically equivalent $\mathbf{L^{3-}}$ ligand, one third of the coordinated NO_3^- ion, two coordinated H_2O molecules, and one coordinated DMF molecule. It adopts a twelve nuclear $Ba_{12}(COO)_{18}(NO_3)_2$ cluster, with two NO_3^- ions connecting to six Ba atoms in the inner ring, and another six Ba atoms in the outer ring. As shown in Figure 1, Ba1 is nine-coordinated by nine oxygen atoms: six oxygen atoms (O1–O6) from four different $\mathbf{L^{3-}}$ ligands, two oxygen atom (O7–O8) from NO_3^- ions, and one oxygen atom (O9) from coordinated DMF molecules (Figure 1a). The average Ba1–O distance is 2.888 Å. Six identical Ba1 are connected by two NO_3^- ions and six carboxylates to form an octahedral configuration (Figure 1c). Ba2 is eight-coordinated by eight oxygen atoms, six oxygen atoms (O10–O15) from five different $\mathbf{L^{3-}}$ ligands, and two oxygen atom (O16–O17) from two coordinated H_2O molecules (Figure 1b). The average Ba2–O distance is 2.756 Å. Six identical Ba2 are connected by twelve carboxylates to form a positive hexadole ring with a distance of 6.323 Å between adjacent two Ba2 and a distance of 12.641 Å between diagonal Ba2 (Figure 1d). The octahedron formed by six Ba1 is embedded in the six Ba2-formed six-membered rings by carboxylic oxygen to form a twelve nuclear barium cluster (Figure 1e). This is the first twelve nuclear barium cluster that is constructed from an amino functionalized ligand, which enrichs the structure of coordination chemistry. Every $Ba_{12}(COO)_{18}(NO_3)_2$ cluster connects to eighteen planar triangular $\mathbf{L^{3-}}$ ligands with lower symmetry, and each $\mathbf{L^{3-}}$ ligand connects to three $Ba_{12}(COO)_{18}(NO_3)_2$ clusters to form a 12-c net. Alternatively, this 12-c network can also be described as a three-dimensional network formed by corners sharing of rhombic cages (Figure 1j); the rhombic cages are defined by eight $Ba_{12}(COO)_{18}(NO_3)_2$ clusters at the corners and twelve $\mathbf{L^{3-}}$ ligands on the surface. From the viewpoint of topology, we can simplify the $[Ba_{12}(COO)_{18}(NO_3)_2]$ units into eighteen connected nodes and simplify the $\mathbf{L^{3-}}$ ligand into three connected nodes. Thus, the **UPC-33** adopts a classical ***fcu*** architecture with a topological point symbol of $\{3^{24}\cdot4^{36}\cdot5^6\}$ (Figure 1f–i).

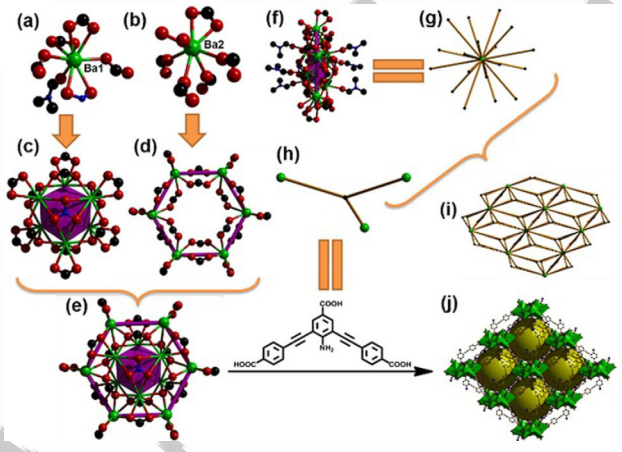

Figure 1. (a) and (b) Coordination environment of Ba1 and Ba2; (c) and (d) The octahedral configuration of Ba1 and the six-membered ring of Ba2; (e) and (f) The octahedron is embedded in the six-membered ring; (g) and (h) The simplified model of $Ba_{12}(COO)_{18}(NO_3)_2$ cluster and $\mathbf{H_3L}$; (i) The topological structure of **UPC-33**; (j) The cage structure with 2D open channels of **UPC-33**.

The volume of the rhombic cage is 7906.0 $Å^3$. **UPC-33** has two open diamond windows in the cage with 9.54×12.93 Å (atom to atom distance) viewed along the [1 0 0] and [0 1 0] direction. Using the SQUEEZE program in the PLATON[23] software package to subtract the solvent contribution, the calculated solvent availability of the **UPC-33** is 55.8% (15112.0 $Å^3$ out of the 27064.0 $Å^3$ unit cell volume), and 1541 electrons were removed from the unit-cell contents. In the $R\bar{3}$ space group, the asymmetric unit is 1/18 of the unit cell, so the asymmetric unit would have contributed 1541/18 = 85.6 electrons, corresponding to one DMF molecule (40 electrons), one C_2H_5OH molecule (26 electrons), and two H_2O molecules (20 electrons).

Gas adsorption and separation

The establishment of permanent porosities is one of the important goals in MOF research. The as-synthesized crystals of **UPC-33** were exchanged three times with dry acetone. The acetone-exchanged samples were degassed at 353 K for 12 hours, until the exhaust gas rate was 5 mm Hg min^{-1}, to produce the activated phases of **UPC-33** for gas sorption measurements. As can be seen from Figure S1 (Supporting Information), the active phase is highly crystalline and remains almost identical to its as-synthesized phase. The permanent porosity of **UPC-33** was confirmed by the reversible N_2 sorption measurements at 77 K and 1 bar, which showed a type I adsorption isotherm performance with a saturated adsorption amount of 324 $cm^3 g^{-1}$ (Figure 2). The Brunauer–Emmett–Teller (BET) and Langmuir surface areas are 933.8 and 1230.3 $m^2 g^{-1}$, calculated from the N_2 sorption isotherm. The pore volume is calculated as 0.50 $cm^3 g^{-1}$ for **UPC-33**, smaller than the theoretical pore volume of 0.62 $cm^3 g^{-1}$, which is a typical of the flexible MOF because of the structural contractions during activation. The pore size distribution is determined with NLDFT■■Please define■■ and calculated from N_2 adsorption isotherms at 77 K, corresponding to a pore size of 4.3 Å for **UPC-33**, which

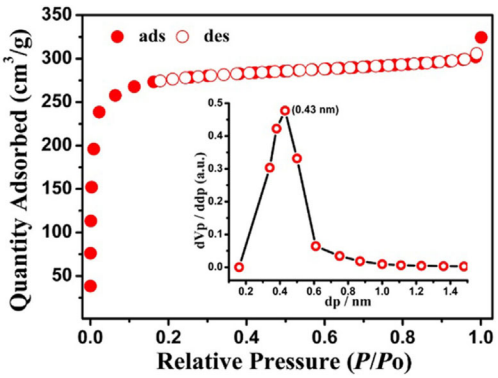

Figure 2. The N_2 sorption isotherms at 77 K and (inset) pore size distribution for **UPC-33**.

Table 1. Single component gas adsorption data for **UPC-33**.

Gas	T [K]	V_{ads} [$cm^3 g^{-1}$]	Amount [$mmol\,g^{-1}$]	Amount [wt.%]	Q_{st} [$kJ\,mol^{-1}$]
CO_2	273	68.1	3.04	13.38	49.92
	298	31.8	1.42	6.25	
CH_4	273	9.7	0.43	0.69	3.56
	298	7.0	0.31	0.50	
C_2H_2	273	65.1	2.91	7.57	15.02
	298	44.3	1.98	5.15	
C_2H_4	273	43.6	1.95	5.46	10.31
	298	31.1	1.39	3.89	
C_2H_6	273	51.8	2.31	6.93	13.86
	298	35.0	1.56	4.68	
C_3H_6	273	114.2	5.10	21.42	48.93
	298	94.3	4.21	17.68	
C_3H_8	273	111.8	4.99	21.96	18.39
	298	93.6	4.18	18.39	

matches well with the kinetic diameters of C3 light hydrocarbons of ~3.3–4.4 Å. Therefore, we speculate that **UPC-33** can be used to separate light hydrocarbons with different kinetic diameters.

Since CO_2 is a dominant component of greenhouse gas and a main contaminant of natural gas, it is meaningful to investigate the capacity of CO_2 and the selectivity of CO_2/CH_4. The low pressure CO_2 adsorption isotherms were measured at 273 and 298 K (Figure 3a, b). The CO_2 uptake of **UPC-33** is 68.1 $cm^3 g^{-1}$ (13.38 wt.%) at 273 K and 31.8 $cm^3 g^{-1}$ (6.25 wt.%) at 298 K under 1 bar, respectively. The adsorption heat (Q_{st}) of CO_2 in **UPC-33** is 49.92 $kJ\,mol^{-1}$ calculated from the Clausius–Clapeyron equation (Figure 3c and Table 1), indicating a strong adsorbate–adsorbant interaction. This value is comparable to known MOFs with $-NH_2$ groups, such as bio-MOF-11 (45 $kJ\,mol^{-1}$), CAU-1 (48 $kJ\,mol^{-1}$), NH_2-MIL-53 (Al) (50 $kJ\,mol^{-1}$), and significantly higher than that of PCN-6 (35 $kJ\,mol^{-1}$), HKUST-1 (35 $kJ\,mol^{-1}$), MOF-5 (34 $kJ\,mol^{-1}$), MIL-53 (Cr) (32 $kJ\,mol^{-1}$), NOTT-140 (25 $kJ\,mol^{-1}$), and UMCM-1 (12 $kJ\,mol^{-1}$).[24] The higher CO_2 uptake capacity of **UPC-33** prompted us to further investigate the selectivity of CO_2 adsorption over CH_4. The predicted CO_2/CH_4 selectivity (for equimolar gas-phase mixtures) by IAST mode at 273 K and 1 bar has been calculated to be 33.12 for **UPC-33** (Figure 3d). It should be noted that these values are lower than those of Mg–MOF-74 (CO_2/CH_4: 105) and SIFSIX-3-Zn (CO_2/CH_4: 231),[25] comparable to UTSA-16 (CO_2/CH_4: 30),[26] and higher than ZIF-79 (CO_2/CH_4: 5.4),[27] SIFSIX-2-Cu (CO_2/CH_4: 5.3),[25] and PCN-88 (CO_2/CH_4: 5.3).[28] This makes **UPC-33** a good candidate for CO_2 capture and separation from natural gas.

Considering the moderate pores in **UPC-33**, its low-pressure C_3H_8 and C_3H_6 uptakes were also measured under 1 bar. As expected, the C_3H_8 and C_3H_6 adsorption amount for **UPC-33** reaches up to 111.8 $cm^3 g^{-1}$ and 114.2 $cm^3 g^{-1}$ at 273 K and

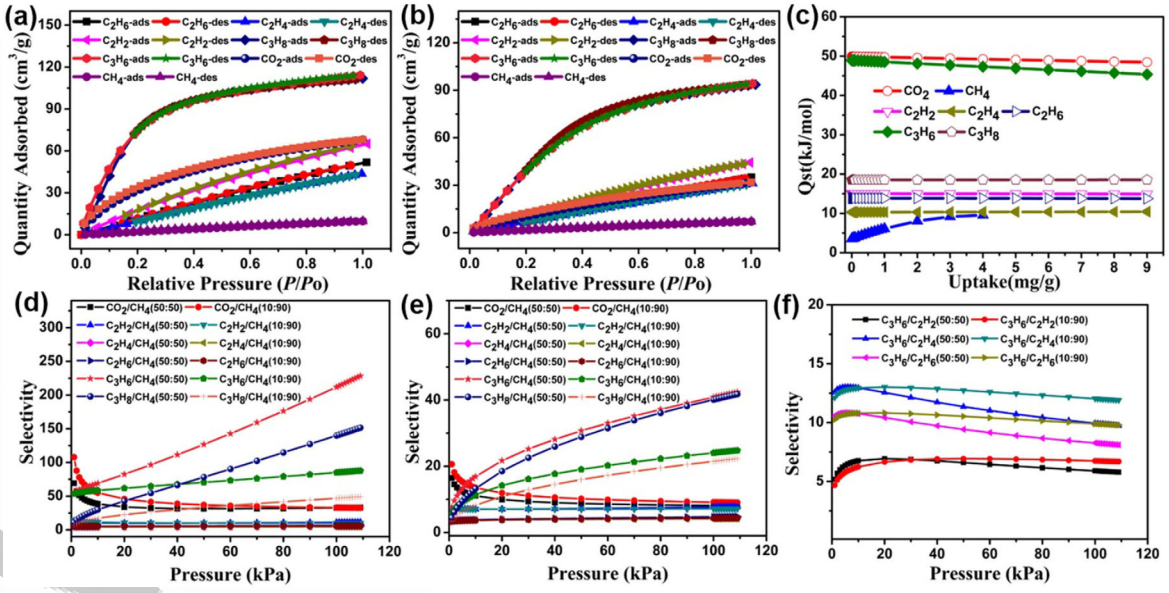

Figure 3. (a) and (b) The CH_4, C_2H_6, C_2H_4, C_2H_2, C_3H_8, and C_3H_6 adsorption isotherms at 273 K and 298 K for **UPC-33**; (c) The Q_{st} for CH_4, C_2H_6, C_2H_4, C_2H_2, C_3H_8, and C_3H_6; (d) and (e) The C_2H_6/CH_4, C_2H_4/CH_4, C_2H_2/CH_4, C_3H_8/CH_4, and C_3H_6/CH_4 selectivity at 298 K, calculated by the IAST method (V/V: 50/50 and 10/90); (f) The C_3H_6/C_2H_2, C_3H_6/C_2H_4, and C_3H_6/C_2H_6 selectivity at 298 K, calculated by the IAST method (V/V: 50/50 and 10/90).

1 bar. In practice, C_3H_8 and C_3H_6 gases are stored at ambient temperature. Therefore, C_3H_8 and C_3H_6 adsorption experiments were carried out at room temperature (298 K). **UPC-33** exhibits an adsorption amount of 93.6 and 94.3 $cm^3 g^{-1}$ for C_3H_8 and C_3H_6 at 298 K and 1 bar, which are slightly lower than that of **UPC-21** (103.0 and 110.1 $cm^3 g^{-1}$),[9] and higher than FJI–C4 (74.7 $cm^3 g^{-1}$ for C_3H_8).[29] Considering its practical application, we also tested the reproducibility of **UPC-33** for C_3H_8 and C_3H_6 storage. About 100 mg of the desensitized sample was loaded onto the ASAP2020-M analyzer, and four cycles of C_3H_8 and C_3H_6 adsorption at 298 K were recorded without the reactivation process between each cycle. The absorption of C_3H_8 and C_3H_6 was only 2.9% and 3.5% lesser after four cycles, indicating that **UPC-33** was promising in refillable C_3H_8 and C_3H_6 storage (Figure 4a, b).

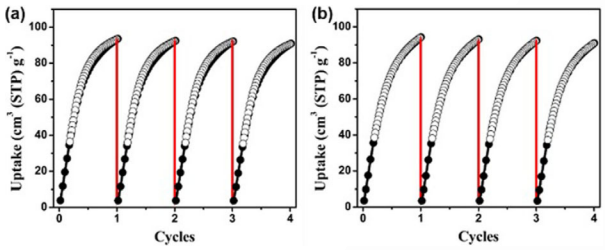

Figure 4. Cycles of C_3H_8 (a) and C_3H_6 (b) adsorption for **UPC-33** at 298 K.

The small pore size and inherent permanent porosity of **UPC-33** have prompted us to investigate the potential application of light hydrocarbons separation. Single component gas sorption isotherms of **UPC-33** for various light hydrocarbons (CH_4, C_2H_2, C_2H_4, and C_2H_6) were performed at both 273 and 298 K. As expected, **UPC-33** can take up a large amount of C_2H_6 (51.8 $cm^3 g^{-1}$), C_2H_4 (43.6 $cm^3 g^{-1}$), and C_2H_2 (65.1 $cm^3 g^{-1}$), but a small amount of CH_4 (9.7 $cm^3 g^{-1}$) at 273 K and 1 bar (Figure 3a). It should be noted that the adsorption capacity of **UPC-33** for C_2H_6 (35.0 $cm^3 g^{-1}$), C_2H_4 (31.1 $cm^3 g^{-1}$), C_2H_2 (44.3 $cm^3 g^{-1}$), and CH_4 (7.0 $cm^3 g^{-1}$) are comparable to that of UTSA-35a[8] and UTSA-36a[15] at 298 K and 1 bar (Figure 3b). The magnitude of the adsorption enthalpies reveals the affinity of the pore surface toward adsorbents, which plays a significant part in determining the selectivity of adsorption.[30] To evaluate the affinity of this light hydrocarbons in **UPC-33**, the adsorption heat is calculated by the Clausius–Clapeyron equation. The adsorption enthalpy of CH_4, C_2H_2, C_2H_4, C_2H_6, C_3H_6, and C_3H_8 are 3.56, 15.02, 10.31, 13.86, 48.93, and 18.52 kJ mol^{-1} at zero coverage, respectively (Figure 3c and Table 1).

The C_3 light hydrocarbons with higher adsorption enthalpy [$Q_{st}(C_3H_6) > Q_{st}(C_3H_8) > Q_{st}(C_2H_2) > Q_{st}(C_2H_6) > Q_{st}(C_2H_4) > Q_{st}(CH_4)$] may provide a stronger affinity for the skeleton, which results in preferential adsorption of these gases on the skeleton of **UPC-33**. Thus, it may have a high selectivity for C_3 light hydrocarbons relative to CH_4. Therefore the potential for separation of CH_4 from C_3 light hydrocarbons is appraised by ideal solution adsorbed theory (IAST) for binary equimolar components (Figure 3d). At 1 bar and 273 K, the selectivities of C_3H_8 and C_3H_6 with respect to CH_4 are 151.50 and 228.34, which are higher than C_2H_2, C_2H_4, and C_2H_6 to CH_4 of 11.36, 5.32, and 6.64, respectively. It should be noted that these values are lower than FJI-C4 (293.4 for C_3H_8/CH_4),[29] but greatly higher than UPC-21 (75 for C_3H_6/CH_4, 67 for C_3H_8/CH_4),[9] or FJI-C1 (78.7 for C_3H_8/CH_4).[31] The results indicate that **UPC-33** is a prospective absorbent for effectively selective adsorptive separation of CH_4 from C_3 hydrocarbons at 273 K. The high adsorption selectivity of C_3/CH_4 can be attributed to the narrow pore size distribution of **UPC-33** to match the kinetic diameter of C_3 light hydrocarbon, resulting in its high C_3/CH_4 sieving effects. Meanwhile, the selectivity of C_3H_6 to C_2H_2, C_2H_4, and C_2H_6 was 10.83, 13.00, and 6.93 at 1 bar and 273 K, respectively. These values are higher than the selectivity of C_3H_8 with respect to C_2H_2, C_2H_4, and C_2H_6 that are 4.84, 8.17, and 6.79, which means that **UPC-33** can also selectively adsorb C_3H_6 from C_2 hydrocarbons at 273k. Although the selectivity decreases at room temperature, **UPC-33** can still effectively separate light hydrocarbons (Figure 3d–f and Table 2).

Table 2. Adsorption selectivity of hydrocarbon at 1 bar for different molar fraction of binary mixtures.

Binary gas mixtures	Molar fraction	Selectivity (273 K)	Selectivity (298 K)
CO_2/CH_4	50:50	33.12	8.09
	10:90	32.70	9.04
C_2H_2/CH_4	50:50	11.36	7.78
	10:90	9.94	7.19
C_2H_4/CH_4	50:50	5.32	4.48
	10:90	4.78	4.18
C_2H_6/CH_4	50:50	6.64	4.80
	10:90	5.78	4.34
C_3H_6/CH_4	50:50	228.34	42.40
	10:90	87.69	24.76
C_3H_8/CH_4	50:50	151.50	41.77
	10:90	49.18	22.30
C_3H_6/C_2H_2	50:50	10.83	3.80
	10:90	10.82	3.81
C_3H_6/C_2H_4	50:50	13.00	5.70
	10:90	13.01	5.84
C_3H_6/C_2H_6	50:50	6.93	4.90
	10:90	6.90	5.31
C_3H_8/C_2H_2	50:50	4.84	3.78
	10:90	5.05	3.71
C_3H_8/C_2H_4	50:50	8.17	5.66
	10:90	8.62	5.61
C_3H_8/C_2H_6	50:50	6.79	4.88
	10:90	7.20	5.12

Knoevenagel condensation reaction

The excellent stability of **UPC-33** for heat, together with the presence of $-NH_2$ group decorated channels and optimized pores satisfy the essential prerequisites for the framework as a heterogeneous catalyst. It has been demonstrated that frameworks constructed with barium(II) ions can catalyze many organic reactions, such as cyanosilylation reactions.[32] Here, we have explored the heterogeneous catalytic activity of **UPC-33** to Knoevenagel reactions involving malononitrile and aromatic aldehydes to give benzylidene malononitrile (Table 3), which

Table 3. Knoevenagel reactions catalyzed by **UPC-33**.

Entry[a]	R	*t* [h]	Yield [%][b]
1	4-NO_2Ph	5	98.2
2	4-MePh	5	93.4
3	Ph	5	89.0
4	4-FPh	5	86.1
5	4-PhPh	5	83.1
6	1-naphthyl	5	80.3
7	4-PhOPh	5	53.8
8	4-MeOPh	5	36.2

[a] Reaction conditions: activated sample **UPC-30** (10 wt.%), an aldehyde (1.0 mmol), malononitril (1.0 mmol, 0.066 g), CH_2Cl_2 (3 mL), room temperature. [b] GC yield.

exhibits a wide scope of important chemical intermediate properties.

In general, a mixture of 1.0 mmol of aldehyde, and 1.0 mmol of malononitrile in CH_2Cl_2 (3 mL) were placed in a round-bottom flask and stirred at room temperature in the presence of **UPC-33** (10 wt.%). The reaction was monitored by TLC, and the reaction was completed within 5 h. Next, the reaction mixture was filtered and washed several times with CH_2Cl_2 to recover the catalyst. The filtrate was dried over Na_2SO_4. The recovered catalyst can be reused after heating at 100 °C under vacuum for 6 h, without loss of activity. The PXRD of the recovered catalyst confirms that the integrity of the framework is maintained even after three reaction cycles (Figure S1). Table 3 summarizes the results of the diverse substrates. As a control experiment, the catalyst was removed after 30 min, which resulted in complete shutdown of the reaction as monitored by using GC-MS (Figure S4). The Knoevenagel condensation yield of benzaldehyde and malononitrile reached 98.2% at room temperature after 5 hours. It should be noted that these values are comparable to PCN-124 (99%),[33] Cz-MOF (99%),[34] and PCP-1 (96%),[35] which makes **UPC-33** a candidate for the C–C coupling reaction. The aromatic aldehydes with bulky and electron-donating groups reduce the reaction rate and yield (Table 3, entries 7 and 8), which are not suitable for the framework cavity.

The catalytic mechanism is similar to that of proposed by Zhang.[36] In the first step, the active sites (amino groups) in the pores of UPC-33 reacted with benzaldehyde to form the imine intermediate (benzaldimine). In the second step, the active site was regenerated after the reaction of malononitrile and the benzaldimine (Figure 5).

Conclusions

In conclusion, we have developed and characterized a novel microporous Ba-MOF **UPC-33** based on pre-designed amino-functionalized ligands. **UPC-33** exhibits high adsorption heat of CO_2 (49.92 kJ mol^{-1}) and selectivity of CO_2/CH_4 (8.09). **UPC-33** has the right pore size to maximize the interaction between the gas and framework, so it exerts a high separation selectivity for C_3 light hydrocarbons relative to CH_4 (228.34, 151.40 for C_3H_6/CH_4, C_3H_8/CH_4 at 273 k and 1 bar) and can selectively

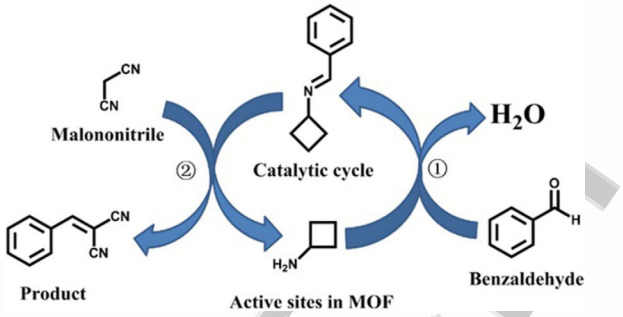

Figure 5. Catalytic reaction mechanism for the Knoevenagel condensation.

adsorb absorb C_3H_6 from C_2 hydrocarbons. These results indicate that **UPC-33** may be a promising candidate for fuel gas purification and light hydrocarbon separation in the near future. In addition, the presence of Lewis basic $-NH_2$ groups allows **UPC-33** to act as a catalyst for size and electronically selective Knoevenagel condensation reactions. Benefitting from the straightforward design of MOFs with modifiable performances, we are developing customizable adsorbents for specific gas separations and exploring heterogeneous catalysts for catalyze organic reactions.

Experimental Section

Materials and methods

All chemical reagents are available from commercial sources and can be used without further purification. The **H_3L** was synthesized by Sonogashira coupling reaction and then hydrolyzed with dilute HCl. (Scheme S1 in the Supporting Information). The ^{1}H NMR spectrum is recorded on a 400 MHz Varian INOVA spectrometer and referenced to the residual solvent peak. Powder X-ray diffraction measurements of **UPC-33** are performed on an analytical X-Pert pro diffractometer with $Cu_{K\alpha}$ radiation ($\lambda = 1.54184$ Å). Thermogravimetric analysis (TGA) are performed on a Mettler Toledo TGA under N_2 flow and heated from room temperature to 900 °C (at 10 °C min^{-1}). Elemental analyses (C, H, N) are obtained on a PerkinElmer 240 elemental analyzer. The photoluminescence (PL) spectrum is measured using Hitachi F-7000 fluorescence spectrophotometer at room temperature. Infrared (IR) spectroscopy spectra are collected on a Nicolet 330 FTIR spectrometer in the 4000–400 cm^{-1} region. The gas adsorption isotherm is performed on the surface area analyzer Micromeritics ASAP-2020.

Synthesis of UPC-33

UPC-33 was prepared by the solvothermal reaction. A mixture of H_3L (6.0 mg, 0.016 mmol) and $Ba(NO_3)_2 \cdot 6H_2O$ (60.0 mg, 0.17 mmol) was ultrasonically dissolved in DMF: C_2H_5OH: H_2O (V:V:V = 5:2:1, 2 mL) solution in 10 mL vial. The mixture was heated at 100 °C for 4300 min, and then cooled to room temperature. Light yellow block crystals were acquired with a yield of 35% based on **H_3L**. FTIR (KBr): $\tilde{\nu} = 3465$ (w), 3387 (s), 1668 (s), 582 (s), 1515 (w), 1381 (s), 1314 (w), 1247 (w), 1095 (s), 856 (m), 789 (w), 722 cm^{-1} (w); elemental analysis calcd (%) for $C_{33}H_{38}Ba_2N_{3.33}O_{13}$: C 41.14, H 3.95, N, 4.84; found: C 41.36, H 3.72, N 4.79.

Crystal structure determinations

The crystallographic data of **UPC-33** was collected on an Agilent Xcalibur Eos Gemini diffractometer with (Cu) X-ray Source ($Cu_{K\alpha}$ $\lambda = 1.54184$ Å). Absorption correction was carried out by multi-scan method, using the SADABS program to apply the empirical absorption correction.[37] The structures were solved by direct methods and refined by the full-matrix least-squares method on F^2, and all non-hydrogen atoms were refined with anisotropic thermal parameters.[38] All the hydrogen atoms attached to carbon atoms were placed in calculated positions and refined using the riding model, and the water hydrogen atoms were located from the difference maps. In **UPC-33**, the final structure has a large number of void volumes containing a plurality of residual electron density peaks, which can be attributed to the disordered solvent molecules, and could not be crystallographically defined satisfactorily. According to crystallographic data combined with elemental and thermogravimetric analyses, the solvent molecules were proposed to be one DMF, one EtOH, and two H_2O molecules for **UPC-33**. The crystal and refinement parameters are listed in Table S1. CCDC 1570710 (**UPC-33**) contains the supplementary crystallographic data for this paper. These data are provided free of charge by The Cambridge Crystallographic Data Centre.

Gas sorption measurements

Gas adsorption–desorption measurements of N_2, CO_2, CH_4, C_3H_6, C_3H_8, C_2H_2, C_2H_6, and C_2H_4 on **UPC-33** were collected on the Micromeritics ASAP 2020 surface area and pore size analyzer. The temperatures of 77 K, 273 K, and 298 K were maintained with a liquid nitrogen bath, an ice-water bath, and under room temperature, respectively. The measurements were carried out at 77 K (N_2), 273 K (CO_2, CH_4, C_3H_6, C_3H_8, C_2H_2, C_2H_6, and C_2H_4), and 298 K (CO_2, CH_4, C_3H_6, C_3H_8, C_2H_2, C_2H_6, and C_2H_4). The Brunauer–Emmett–Teller (BET) surface area and pore size distribution data were calculated from the N_2 adsorption isotherms at 77 K based on a non-local density functional theory (NLDFT) model in the Micromeritics ASAP2020 software package (assuming a slit pore geometry).

Acknowledgements

We are grateful for financial support from the National Natural Science Foundation of China (Grant Nos. 21371179, 21571187, 21701187), Taishan Scholar Foundation (ts201511019).

Conflict of Interest

The authors declare no conflict of interest.

Keywords: gas storage · ideal solution adsorbed theory (IAST) · light hydrocarbons · metal-organic frameworks · selectivity separation

[1] J. R. Li, J. Sculley, H. C. Zhou, *Chem. Rev.* **2012**, *112*, 869 – 932.
[2] H. Wu, Q. Gong, D. H. Olson, J. Li, *Chem. Rev.* **2012**, *112*, 836 – 868.
[3] B. Li, H. M. Wen, H. L. Wang, H. Wu, M. Tyagi, T. Yildirim, W. Zhou, B. L. Chen, *J. Am. Chem. Soc.* **2014**, *136*, 6207 – 6210.
[4] B. L. Chen, N. W. Ockwig, A. R. Millward, D. S. Contreras, O. M. Yaghi, *Angew. Chem. Int. Ed.* **2005**, *44*, 4745 – 4749; *Angew. Chem.* **2005**, *117*, 4823 – 4827. ■ ■pg. nos. were wrong. please check corrected pages■ ■
[5] a) Y. B. He, R. Krishna, B. L. Chen, *Energy Environ. Sci.* **2012**, *5*, 9107 – 9120; b) H.-R. Fu, J. Zhang, *Inorg. Chem.* **2016**, *55*, 3928 – 3932; c) H.-R. Fu, J. Zhang, *Chem. Eur. J.* **2015**, *21*, 5700 – 5703.
[6] K. Srinivasu, S. K. Ghosh, *J. Phys. Chem. C* **2011**, *115*, 16984 – 16991.
[7] E. D. Bloch, W. L. Queen, R. Krishna, J. M. Zadrozny, C. M. Brown, J. R. Long, *Science* **2012**, *335*, 1606 – 1610.
[8] Y. He, Z. Zhang, S. Xiang, F. R. Fronczek, R. Krishna, B. Chen, *Chem. Commun.* **2012**, *48*, 6493 – 6495.
[9] M. H. Zhang, X. L. Xin, Z. Y. Xiao, R. M. Wang, L. L. Zhang, D. F. Sun, *J. Mater. Chem. A.* **2017**, *5*, 1168 – 1175.
[10] T. L. Hu, H. Wang, B. Li, R. Krishna, H. Wu, W. Zhou, Y. Zhao, Y. Han, X. Wang, W. Zhu, Z. Yao, S. C. Xiang, B. L. Chen, *Nat. Commun.* **2015**, *6*, 7328.
[11] H. Xu, J. F. Cai, S. C. Xiang, Z. J. Zhang, C. D. Wu, X. T. Rao, Y. J. Cui, Y. Yang, R. Krishna, B. L. Chen, G. D. Qian, *J. Mater. Chem. A.* **2013**, *1*, 9916 – 9921.
[12] Z. J. Lin, T. F. Liu, Y. B. Huang, J. Lu, R. Cao, *Chem. Eur. J.* **2012**, *18*, 7896 – 7902.
[13] J. R. Li, R. J. Kuppler, H. C. Zhou, *Chem. Soc. Rev.* **2009**, *38*, 1477 – 1504.
[14] A. H. Assen, Y. Belmabkhout, K. Adil, P. M. Bhatt, D. X. Xue, H. Jiang, M. Eddaoudi, *Angew. Chem. Int. Ed.* **2015**, *54*, 14353 – 14358; *Angew. Chem.* **2015**, *127*, 14561 – 14566.
[15] Y. B. He, Z. J. Zhang, S. C. Xiang, F. R. Fronczek, R. Krishna, B. L. Chen, *Chem. Eur. J.* **2012**, *18*, 613 – 619.
[16] Y. B. He, W. Zhou, R. Krishna, B. L. Chen, *Chem. Commun.* **2012**, *48*, 11813 – 11831.
[17] A. M. Bohnsack, I. A. Ibarra, P. W. Hatfield, J. W. Yoon, Y. K. Hwang, J. S. Chang, S. M. Humphrey, *Chem. Commun.* **2011**, *47*, 4899 – 4901.
[18] A. H. Chughtai, N. Ahmad, H. A. Younus, A. Laypkov, F. Verpoort, *Chem. Soc. Rev.* **2015**, *44*, 6804 – 6849.
[19] J. Li, H. R. Fu, J. Zhang, L. S. Zheng, J. Tao, *Inorg. Chem.* **2015**, *54*, 3093 – 3095.
[20] H. R. Fu, F. Wang, J. Zhang, *Dalton Trans.* **2015**, *44*, 2893 – 2896.
[21] J. Li, Y. Guo, H. R. Fu, J. Zhang, R. B. Huang, L. S. Zheng, J. Tao, *Chem. Commun.* **2014**, *50*, 9161 – 9164.
[22] X. Duan, Y. B. He, Y. J. Cui, Y. Yang, R. Krishna, B. L. Chen, G. D. Qian, *RSC Adv.* **2014**, *4*, 23058 – 23063.
[23] A. L. Spek, PLATON, A multipurpose crystallographic tool; Utrecht University: The Netherlands, **2001**.
[24] a) J. An, J. S. Geib, N. L. Rosi, *J. Am. Chem. Soc.* **2010**, *132*, 38 – 39; b) X. Si, C. Jiao, F. Li, J. Zhang, S. Wang, S. Liu, Z. Li, L. Sun, F. Xu, Z. Gabelica, C. Schick, *Energy Environ. Sci.* **2011**, *4*, 4522 – 4527; c) S. Couck, J. F. M. Denayer, G. V. Baron, T. Rémy, J. Gascon, F. Kapteijn, *J. Am. Chem. Soc.* **2009**, *131*, 6326 – 6327; d) J. An, N. L. Rosi, *J. Am. Chem. Soc.* **2010**, *132*, 5578 – 5579; e) Z. Zhao, Z. Li, Y. S. Lin, *Ind. Eng. Chem. Res.* **2009**, *48*, 10015 – 10020; f) S. Bourrelly, P. L. Llewellyn, C. Serre, F. Millange, T. Loiseau, G. Férey, *J. Am. Chem. Soc.* **2005**, *127*, 13519 – 13521; g) C. Tan, S. Yang, N. R. Champness, X. Lin, A. J. Blake, W. Lewis, M. Schröder, *Chem. Commun.* **2011**, *47*, 4487 – 4489; h) B. Mu, P. M. Schoenecker. K. S. Walton, *J. Phys. Chem. C* **2010**, *114*, 6464 – 6471.
[25] P. Nugent, Y. Belmabkhout, S. D. Burd, A. J. Cairns, R. Luebke, K. Forrest, T. Pham, S. Ma, B. Space, L. Wojtas, M. Eddaoudi, M. J. Zaworotko, *Nature* **2013**, *495*, 80 – 84.
[26] S. Xiang, Y. He, Z. Zhang, H. Wu, W. Zhou, R. Krishna, B. Chen, *Nat. Commun.* **2012**, *3*, 954.
[27] A. Phan, C. J. Doonan, F. J. Uribe-Romo, C. B. Knobler, M. O'Keeffe, O. M. Yaghi, *Acc. Chem. Res.* **2010**, *43*, 58 – 67.
[28] J. R. Li, J. Yu, W. Lu, L. B. Sun, J. Sculley, P. B. Balbuena, H. C. Zhou, *Nat. Commun.* **2013**, *4*, 1538.
[29] L. Li, X. S. Wang, J. Liang, Y. B. Huang, H. F. Li, Z. J. Lin, R. Cao, *ACS Appl. Mater. Interfaces* **2016**, *8*, 9777 – 9781.
[30] Y. Y. Yang, Z. J. Lin, T. T. Liu, J. Liang, R. Cao, *CrystEngComm* **2015**, *17*, 1381 – 1388.
[31] Y. B. Huang, Z. J. Lin, H. R. Fu, F. Wang, M. Shen, X. S. Wang, R. Cao, *ChemSusChem* **2014**, *7*, 2647 – 2653.
[32] F. L. Liu, Y. W. Xu, L. M. Zhao, L. L. Zhang, W. Y. Guo, R. M. Wang, D. F. Sun, *J. Mater. Chem. A* **2015**, *3*, 21545 – 21552.
[33] J. Park, J. R. Li, Y. P. Chen, J. M. Yu, A. A. Yakovenko, Z. U. Wang, L. B. Sun, P. B. Balbuena, H. C. Zhou, *Chem. Commun.* **2012**, *48*, 9995 – 9997.

[34] X. L. Li, B. Y. Zhang, Y. H. Fang, W. J. Sun, Z. Y. Qi, Y. C. Pei, S. Y. Qi, P. Y. Yuan, X. C. Luan, T. W. Goh, W. Y. Huang, *Chem. Eur. J.* **2017**, *23*, 4266 – 4270.
[35] R. K. Das, A. Aijaz, M. K. Sharma, P. Lama, P. K. Bharadwaj, *Chem. Eur. J.* **2012**, *18*, 6866 – 6872.
[36] Y. F. Yu, X. J. Wu, M. T. Zhao, Q. L. Ma, J. Z. Chen, B. Chen, Me. Sindoro, J. Yang, S. K. Han, Q. P. Lu, H. Zhang, *Angew. Chem. Int. Ed.* **2017**, *56*, 578 – 581; *Angew. Chem.* **2017**, *129*, 593 – 596.
[37] G. M. Sheldrick, SADABS, Program for Empirical Absorption Correction of Area Detector Data; Göttingen University, Germany, **1996**.
[38] a) G. M. Sheldrick, SHELXS-97, Program for Crystal Structure Solution, Göttingen University, Germany, **1997**; b) G. M. Sheldrick, SHELXL-97, Program for Crystal Structure Refinement, Göttingen University, Germany, **1997**.

Manuscript received: September 29, 2017
Accepted manuscript online: October 24, 2017
Version of record online: ■■ ■■, 0000

FULL PAPER

Metal-organic Frameworks

W. Fan, Y. Wang, Q. Zhang, A. Kirchon, Z. Xiao, L. Zhang, F. Dai, R. Wang, D. Sun**

■■ – ■■

An Amino-Functionalized Metal-Organic Framework, Based on a Rare $Ba_{12}(COO)_{18}(NO_3)_2$ Cluster, for Efficient $C_3/C_2/C_1$ Separation and Preferential Catalytic Performance

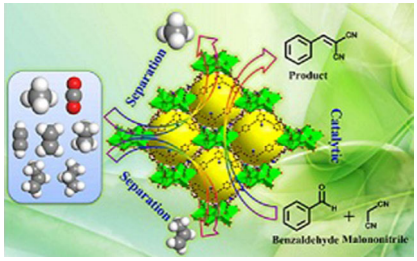

Easy separation: An amino-functionalized and $Ba_{12}(COO)_{18}(NO_3)_2$ based microporous metal – organic framework (**UPC-33**) exhibits high separation selectivity for C3 light hydrocarbons with respect to CH_4 and effectively catalyze Knoevenagel condensation reactions.

Sun, Zhang et al. on a barium #metalorganicframework for hydrocarbon separation and catalysis SPACE RESERVED FOR IMAGE AND LINK

Share your work on social media! *Chemistry - A European Journal* has added Twitter as a means to promote your article. Twitter is an online microblogging service that enables its users to send and read text-based messages of up to 140 characters, known as "tweets". Please check the pre-written tweet in the galley proofs for accuracy. Should you or your institute have a Twitter account, please let us know the appropriate username (i.e., @accountname), and we will do our best to include this information in the tweet. This tweet will be posted to the journal's Twitter account @ChemEurJ (follow us!) upon online publication of your article, and we recommended you to repost ("retweet") it to alert other researchers about your publication.

Please check that the ORCID identifiers listed below are correct. We encourage all authors to provide an ORCID identifier for each coauthor. ORCID is a registry that provides researchers with a unique digital identifier. Some funding agencies recommend or even require the inclusion of ORCID IDs in all published articles, and authors should consult their funding agency guidelines for details. Registration is easy and free; for further information, see http://orcid.org/.

Weidong Fan
Yutong Wang
Qian Zhang
Angelo Kirchon
Zhenyu Xiao
Liangliang Zhang
Dr. Fangna Dai
Rongming Wang
Prof. Daofeng Sun http://orcid.org/0000-0003-3184-1841